Marshall University
Marshall Digital Scholar

Theses, Dissertations and Capstones

1-1-2011

Cancer Cachexia and Cardiac Atrophy in the APCmin/+ Mice Model of Colon Cancer

Nandini Durga Prasanna Kumar Manne
kumar.vetdoc@gmail.com

Follow this and additional works at: http://mds.marshall.edu/etd

 Part of the Cardiology Commons, and the Oncology Commons

Recommended Citation
Manne, Nandini Durga Prasanna Kumar, "Cancer Cachexia and Cardiac Atrophy in the APCmin/+ Mice Model of Colon Cancer" (2011). *Theses, Dissertations and Capstones.* Paper 103.

This Thesis is brought to you for free and open access by Marshall Digital Scholar. It has been accepted for inclusion in Theses, Dissertations and Capstones by an authorized administrator of Marshall Digital Scholar. For more information, please contact zhangj@marshall.edu.

CANCER CACHEXIA AND CARDIAC ATROPHY IN THE *APC*$^{Min/+}$ MICE MODEL OF COLON CANCER

A thesis submitted to the

Graduate College of Marshall University

in partial fulfillment of the requirements for the degree of

Master of Science

Department of Biological Sciences

by

Nandini Durga Prasanna Kumar Manne

Approved by

Dr. Eric R Blough, Committee Chairperson

Dr. David S. Mallory

Dr. Bin Wang

Marshall University

July 2011

ACKNOWLEDGMENTS

It is my immense pleasure to thank my thesis advisor and committee chair Dr. Eric R. Blough whose thoughts are invaluable in succeeding to have this thesis work done. He always encouraged me and gave me right direction in working with my research project. Thank you very much Eric for your guidance, support and encouragement throughout my graduate studies career at Marshall University. I hope everyone gets to be blessed with the kind of advisor that I have now. I would like to thank Dr. David S. Mallory for his valuable suggestions and comments on the thesis work. He is very good teacher and I always loved his classes in the Animal Physiology course. I also would like to thank Dr. Bin Wang for her valuable thoughts about the research work and comments on the thesis work. I would like to extend my deepest gratitude to my esteemed colleagues Dr. Kevin Rice, Dr. Arun Kumar, Dr. Miaozong Wu, Siva Nalabotu, Srinu Thulluri, Anjaiah Katta, Madhukar Kolli, Hari Addagarla, Satya Paturi, Ravi Arvapalli, Sudarsanam Kundla, Radhakrishna Para, Geeta Nandyala, Sravanthi Bodapati and Eli Shleser at the Center for Diagnostic Nanosystems for all of their support and encouragement. I would like to extend my heartfelt thanks to Sunil Kakarla without whose encouragement I would have not been to Marshall University. I am so grateful to my parents Prasad Babu Manne and Bhavani Manne, my sister and brother-in-law Deepthi and Sharat and my uncles Venkat Raju, Sailendra and Sai for all of their help and support in achieving this goal of getting Master's degree in United States. I would like to extend my gratitude to my class mates back at India who helped me at every step in my studies.

TABLE OF CONTENTS

ABBREVIATIONS

4EBP1	4E-binding protein1
APC	Adenomatous polyposis coli
AMPK	5' adenosine monophosphate-activated protein kinase
ANOVA	Analysis of variance on ranks
BSA	Bovine serum albumin
ECL	Enhanced chemiluminiscence
EIF4E	Eukaryotic translation initiation factor 4E
IOD	Integrated Optical Densities
MHC	Myosin heavy chain
Min	Multiple intestinal neoplasia
mTOR	Mammalian Target of Rapamycin
NCI	National Cancer Institute
Nf-kB	Nuclear factor - kappaB
p70S6k	70 kDa ribosomal S6 kinase
PKB	Protein kinase B
S6rp	S6 Ribosomal Protein
SEM	Standard Error Mean
SDS-PAGE	Sodium Dodecyl Sulfate-Polyacrylamide Gel Electrophoresis
Stat-3	Signal transducers and activators of transcription protein
TBS	Tris buffered saline
TBST	Tris buffered saline with 0.5% tween

LIST OF TABLES

LIST OF FIGURES

ABSTRACT

Cancer cachexia is a muscle wasting condition that occurs in response to a malignant growth in the body. Cachexia is associated with heart failure and is estimated to be the immediate cause of death in about a third of all cancer patients. The purpose of this study was to investigate cardiac atrophy in the *Apc*$^{Min/+}$ mouse model of colorectal cancer. Compared to age matched C57BL/6 (BL6) mice, *Apc*$^{Min/+}$ body mass and heart mass were lower at 12 (11.1 ± 4.5% and 7.6 ± 2.8%, respectively) and 20-weeks (26.1 ± 2.5% and 6.0 ± 3.8%, respectively) of age ($P < 0.05$). Immunoblot analysis revealed that these changes in mass were accompanied by increased activation of protein kinase B (Akt Thr 473: 74.4 ± 10.9% and 216.0 ± 19.6% ; Akt Ser 308: 161.6 ± 31.7% and 367.4 ± 41.6% at 12- and 20-weeks, respectively, ($P < 0.05$)), mammalian target of rapamycin (mTOR Ser2448: 23.2 ± 13.2% and 44.0 ± 16.4% at 12- and 20-weeks, respectively, ($P < 0.05$)), 5' adenosine monophosphate-activated protein kinase (AMPK: 19.6 ± 5.2% and 22.5 ± 5.5% at 12- and 20-weeks, respectively, ($P < 0.05$)) and elevated levels of the autophagy regulator beclin1 (4.7 ± 3.3% and 9.5 ± 3.0% at 12- and 20-weeks, respectively, ($P < 0.05$)). No evidence of increased cardiac apoptosis, protein ubiquitination or activation of cardiac caspases or calpains was noted. Taken together, these data suggest that the cardiac atrophy that occurs in the 12- and 20-week old *Apc*$^{Min/+}$ mouse is relatively modest compared to that seen with other tumor models [1] and is associated with evidence of increased cardiac autophagy.

Key words: Cancer cachexia; cardiac atrophy; Akt/mTOR; AMPK; autophagy

CHAPTER 1

Introduction

Cancer and heart diseases are the two leading causes of death in the United States. The total number of deaths worldwide due to cancer is estimated to have been greater than 7.5 million in 2008 alone. Deaths from cancer are projected to rise to over 11 million by the year 2030. Colorectal cancer is the third most common type of cancer and it is expected that this disease will claim the lives of almost 50,000 individuals in the United States during 2011.

Cachexia is characterized by generalized muscle wasting accompanied by weakness and anorexia. According to the National Cancer Institute, this life threatening paraneoplastic syndrome is estimated to be the immediate cause of death in 20% to 40% of cancer patients [2]. The $Apc^{Min/+}$ mouse has a nonsense mutation at codon 850 in the *Apc* gene, resulting in a truncated protein product that predisposes these animals to both small and large intestine adenomas [3]. Given that these mice develop a condition analogous to colorectal cancer with subsequent progression into cachectic stage, this model has been widely used as a model for cancer cachexia related studies.

People suffering from cancer are most likely to have multiple co-morbidities. These co-morbidities may include heart failure, pulmonary hypertension, and ischemic heart disease amongst others [4]. The presence of co-morbidity drastically affects the quality of life in cancer patients. With respect to cardiac disease, it is oftentimes difficult to ascertain the cause of heart failure in cancer patients as it is difficult to ascertain whether it may be due to a prevailing condition or if it is due to therapies related to the cancer treatment. Similarly, how cancer cachexia may affect the heart is not well understood.

Cardiac remodeling is the alteration in shape, size or structure of the heart that occurs in response to increased stress [5]. Whether cardiac atrophy occurs during cancer progression in the

Apc$^{Min/+}$ mice heart has, to our knowledge, has not been investigated. Similarly, the molecular mechanism(s) that may be responsible for such changes, if present, are currently unclear.

Purpose

The purpose of this study is to examine if cardiac atrophy occurs and the molecular mechanism(s) that may be responsible for atrophy, if present, during the progression of cancer cachexia in the *Apc*$^{Min/+}$ mouse model of colorectal cancer.

Specific Aims

Colorectal cancer is the third leading cause of cancer deaths in the United States that is estimated to tax the American health care system over $14 billion a year [6]. The costs of this disorder in terms of human suffering are incalculable. Cachexia is oftentimes associated with advanced cancer and is considered to be responsible for close to a third of all cancer-related deaths. Recent data have suggested that cachexia causes atrophy of skeletal muscles through decreased protein synthesis and increases in protein degradation [7]. This decrease in protein synthesis is thought to occur, at least in part, through alterations in the activation of the 5' AMP-activated protein kinase (AMPK), protein kinase B (Akt) and mammalian target of rapamycin (mTOR) signaling. Whether similar events occur in the heart has not been investigated. The primary objective of this study is to determine if cancer cachexia is associated with cardiac atrophy and whether this atrophy, if present, is characterized by alterations in AMPK and Akt/ mTOR pathway signaling. To accomplish this objective we will pursue the following specific aims:

Specific Aim 1:

To determine if the total and phosphorylated levels of proteins in AMPK and Akt/mTOR pathways are altered in hearts of mice with cancer cachexia.

Hypothesis:

Total and phosphorylated levels of proteins in AMPK and Akt/mTOR pathways will be altered in the hearts of mice with cancer cachexia.

Specific Aim 2:

To observe if there is alteration in total protein degradation levels in hearts of mice with cancer cachexia.

Hypothesis:

There will be an increase in total protein degradation in hearts of mice with cancer cachexia compared to that observed in age matched control animals.

CHAPTER 2

Review of Literature

Introduction

A review of the relevant literature concerning this study will be presented. The following areas of interest will be addressed: 1) Regulation of AMPK and Akt/mTOR pathway related proteins in cancer cachexia and 2) Interplay of apoptosis and autophagy in cancer cachexia.

Regulation of AMPK and Akt/mTOR pathway related proteins in cancer cachexia

The 5' adenosine monophosphate-activated protein kinase (AMPK) is an enzyme that is chiefly involved in cellular metabolism and energy balance in the body [8, 9]. The AMPK is a heterotrimer that is composed of three subunits (α, β and γ), each one of which plays a role in activation of the enzyme. The γ subunit of AMPK is responsible for detecting the changes in AMP : ATP ratio [10]. Any physiological or pathological condition that lowers ATP levels causes the γ subunit to bind to the β domain which results in a conformational change. This change in conformation in turn exposes the catalytic domain on α subunit which allows AMPK to be phosphorylated by upstream kinases.

It is thought that the, AMPK is activated primarily due to a change in cellular energy levels although the mechanism of activation may differ depending upon the condition. During conditions of increased stress, a serine threonine kinase called LKB1 activates AMPK by phosphorylation at threonine 172 [11]. Like LKB1, transforming growth factor-β-activated kinase 1 (TAK1) can also phosphorylate AMPK and causes its activation. Although the exact mechanism of activation of AMPK by TAK1 remains unclear, recent data suggest that AMPK is activated by LKB1 through tumor necrosis factor-related apoptosis inducing ligand (TRAIL) [12]. In addition to changes in

ATP levels, AMPK is also activated by via AMP independent mechanisms such as the Ca^{2+}-dependent upstream kinase CaMKKß [13] or by increased leptin levels [14].

Recent studies have shown that AMPK is activated in the skeletal muscle of rats injected with Yoshida AH-130 ascites hepatoma cells or C26 adenocarcinoma cells. In addition to increased AMPK activation, these authors also noted that cachexia was associated with increased expression of muscle-specific ubiquitin ligases and elevations in ubiquitin mediated protein degradation [15]. Other studies have reported that AMPK activation causes protein degradation through autophagy [1]. Whether similar changes may occur in the cachectic has not been investigated.

The mammalian target of rapamycin (mTOR) is a protein that functions as nutrient-sensing signaling molecule in mammalian cells and is involved in regulating cell survival and protein synthesis. mTOR is an upstream molecule for p70S6 kinase (p70S6k) and 4E-binding protein-1 (4EBP1) which are thought to be key regulators of protein synthesis. mTOR through its interaction with raptor and GβL together form the mTORC1 complex which controls the phosphorylation of p70s6k and the eukaryotic initiation factor-4E (EIF4E) binding protein. It is thought that the interaction between raptor and GβL / mTOR is dependent on availability of nutrients [16]. In low nutrient conditions, raptor is phosphorylated by AMPK which results in tight binding between raptor and mTOR [17] and an inhibition of protein translation.

p70s6k is a serine/threonine kinase which is involved in translation of mRNAs containing a terminal oligopolypyrimidine (TOP) track at their 5' end, a process that is thought to be a rate-limiting step in protein synthesis [18]. The phosphorylation of p70s6k is dependent on its interaction with the mTOR-raptor complex although recent data has suggested that Pdk1 may also play a role via the activation of PI3K signaling. 4EBP1 is a downstream target of mTOR which is phosphorylated by mTORC1 complex under nutrient rich conditions [19].

Phosphorylation of 4EBP1 causes release of EIF4E which allows the mRNA to interact fully with the ribosome. However in one study it is shown that inhibition of mTOR signaling by rapamycin causes an increase in EIF4E phosphorylation in human cancer cell line**.** It was shown that phosphorylation of EIF4E is independent of signal from mTORC1 complex and that the signal for its activation comes from the phosphatidylinositol-3 kinase (PI3K) and Mnk-mediated mechanisms [20].

Several studies to date have shown that the mechanisms involved in activation of mTOR are blocked in cancer cachexia. Activation of mTOR by mTOR kinase is dependent on the interaction of raptor and GβL with mTOR. This mutual interaction is dependent on the availability of glucose and amino acids. In people with colorectal cancer the absorption of nutrients in small intestine is impaired and available nutrients may be directed towards the actively growing tumor cells which can deprive the body of essential nutrients and lead to muscle wasting. This condition can lead to AMPK activation and the phosphorylation of raptor. Phosphorylation of raptor causes tight interaction with mTOR and inhibits mTOR kinase activity. As a consequence mTOR goes into an inactive stage with the subsequent inhibition of protein synthesis.

Akt is a serine/threonine protein kinase that is an upstream regulator of mTOR. Akt acts as a key molecule in several metabolic processes such as glucose metabolism, fatty acid metabolism and protein synthesis [21]. When phosphorylated, Akt activates mTOR which in turn phosphorylates EIF4E binding protein and p70s6k causing an increase in protein synthesis. In addition to the regulation of protein synthesis, Akt is also involved in cell survival functions by exerting its effect on anti-apoptotic molecules Bcl-2 and Foxo-1 [22, 23] and in the regulation of nitric oxide production by eNOS [24]. Recently it was shown that activation of Akt causes phosphorylation of Bad that is involved in anti-apoptosis [25].

Although the role of Akt in cancer has been well documented, little is known about how it may be regulated during cancer cachexia. Recently Michelle and colleagues in 2010 proposed that Akt activation is down regulated in quadriceps and epididymal fat of male CD2F1 mice infected by colon-26 adenocarcinoma tumors. These researchers also showed that this down regulation of Akt is accompanied by an increase in expression of atrophy promoting genes Atrogin-1, MuRF-1, and Bnip3 [26]. Other work has suggested that the phosphorylation of Akt in the skeletal muscle of cancer cachectic patients is reduced by almost 55% when compared to levels seen in skeletal muscle obtained from normal patients. Surprisingly, this same group has also reported increases in Akt activation in liver of cachectic patients [27]. Similarly, work in rats with AH-130 hepatoma and in mice transplanted with C26 colon adenocarcinoma has demonstrated that the phosphorylation of Akt and its downstream effectors p70s6k and Gsk3β is increased in the skeletal muscles of cancer afflicted animals when compared to that observed in the non-tumor bearing animals. Whether Akt activation is present in the hearts of cachectic animals has, to our knowledge, not been investigated.

Summary

AMPK, Akt and the Akt effector molecules mTOR and p70s6k are intimately involved in the regulation of protein synthesis and cellular metabolism. The exact mechanism(s) regulating the activity of the molecules and their complex interplay in cancer cachexia remains unclear. Elucidating the differences between normal and cachectic tissue at the molecular level may be beneficial for dietary and pharmacological interventions designed for the treatment of heart failure in cancer cachexia.

Interplay of apoptosis and autophagy in cancer cachexia

Apoptosis and autophagy are the two most common mechanisms that mediate cell death. The fate of cell survival depends on the signals that inhibit apoptotic and autophagy pathways. Autophagy is a catabolic process by which components of a cell are removed by a degradative process involving sequestration of parts of the cytoplasm in a double membrane vesicle to form an autophagosome [28]. During conditions of nutrient starvation autophagy is activated, which results in recycling up the macromolecular structures in autophagolysomes that can be reutilized again leading to cell survival [29]. The activation of autophagy pathway depends mainly on the state of mTOR and AMPK [30]. Rheb is a GTP binding protein that is involved in S6K signaling and in the activation of mTOR when amino acids are present. During the depletion of amino acids the Rheb is dissociated from mTOR and the activation of mTOR is prevented. During cachexia there is a greater depletion of available ATP in the body as a result of which the nutrient sensing molecule AMPKα is activated. Research by Matsui *et al* showed that autophagy is induced by glucose deprivation in cardiac myocytes by activation of AMPKα and inhibition of mTOR. ULK1 a mammalian homologue of the yeast autophagy regulator, Atg1 is a serine/threonine protein kinase which can promote or inhibit autophagy depending upon it phosphorylation status. Like Atg1, ULK1 is required for initiation of autophagy downstream of target of rapamycin. Under nutrient rich conditions mTOR phosphorylates ULK1 at S757 which results in the inhibition of autophagy. Conversely, the phosphorylation of ULK1 at S317 and S777 by AMPK promotes autophagy [31]. Whether cancer cachexia causes cardiac autophagy is not well understood.

Apoptosis or programmed cell death is a mechanism wherein cells die gradually in an orderly fashion. It is thought that apoptosis is regulated by members of Bcl2 family and the caspases [32]. Members of the Bcl2 family have both pro-apoptotic or anti-apoptotic functions [33]. Although Bcl-2 and Bcl-x_L function as antiapoptotic factors, Bax and Bid are pro-apoptotic.

Apoptosis is regulated by both intrinsic and extrinsic signals [34]. The extrinsic pathway is activated when cytokines such as TNF-α bind to the receptors on cell surface [35]. The binding of TNF-α to its receptor results in the recruitment procaspase 8 to the cell membrane, which leads to the formation of a death inducing signaling complex. The activation of intrinsic apoptosis pathway is under the control of mitochondria and is regulated by increases in oxidative stress, cell starvation, or alterations in growth factors concentration [36]. During stressful conditions mitochondria initiate apoptosis by releasing cytochrome c which, in turn, causes the release of apoptotic protease- activating factor (Apaf-1) [37]. Apaf-1, in turn, causes the release of caspase 9 which initiates the activation of other caspases and eventually cell death.

The ubiquitin-proteasome pathway is the main non-lysosomal pathway for protein degradation in eukaryotes [38]. In this process, proteins are ubiquitinated by ubiquitin ligases which results in their being targeted for degradation by the 26S proteasome [39]. Ubiquitination is involved in controlling the cellular concentration of the tumor suppressor p53, Nf-kB and other cell cycle proteins that are known to be involved in the regulation of apoptosis [40]. How cachexia may affect the regulation of cardiac apoptosis has not yet been elucidated.

Summary

Although autophagy is a lysosomal mediated process of cell death, apoptosis is a process of programmed cell death mediated by mitochondrial release of cytochrome c or activation of death receptors. The role that either of these processes may play in cardiac atrophy during cachexia has yet to be investigated.

CHAPTER 3

Cancer cachexia and cardiac atrophy in the *Apc*$^{Min/+}$ mice model of colon cancer

This chapter will be submitted for publication.

ABSTRACT

Cancer cachexia is a muscle wasting condition that occurs in response to a malignant growth in the body. Cachexia is associated with heart failure and is estimated to be the immediate cause of death in about a third of all cancer patients. The purpose of this study was to investigate cardiac atrophy in the *Apc*$^{Min/+}$ mouse model of colorectal cancer. Compared to age matched C57BL/6 (BL6) mice, *Apc*$^{Min/+}$ body mass and heart mass were lower at 12 (11.1 ± 4.5% and 7.6 ± 2.8%, respectively) and 20-weeks (26.1 ± 2.5% and 6.0 ± 3.8%, respectively) of age ($P < 0.05$). Immunoblot analysis revealed that these changes in mass were accompanied by increased activation of protein kinase B (Akt Thr 473: 74.4 ± 10.9% and 216.0 ± 19.6% ; Akt Ser 308: 161.6 ± 31.7% and 367.4 ± 41.6% at 12- and 20-weeks, respectively, ($P < 0.05$)), mammalian target of rapamycin (mTOR Ser2448: 23.2 ± 13.2% and 44.0 ± 16.4% at 12- and 20-weeks, respectively, ($P < 0.05$)), 5' adenosine monophosphate-activated protein kinase (AMPK: 19.6 ± 5.2% and 22.5 ± 5.5% at 12- and 20-weeks, respectively, ($P < 0.05$)) and elevated levels of the autophagy regulator beclin1 (4.7 ± 3.3% and 9.5 ± 3.0% at 12- and 20-weeks, respectively, ($P < 0.05$)). No evidence of increased cardiac apoptosis, protein ubiquitination or activation of cardiac caspases or calpains was noted. Taken together, these data suggest that the cardiac atrophy that occurs in the 12- and 20-week old *Apc*$^{Min/+}$ mouse is relatively modest compared to that seen with other tumor models [1] and is associated with evidence of increased cardiac autophagy.

Key words: Cancer cachexia; cardiac atrophy; Akt/mTOR; AMPK; autophagy

INTRODUCTION

Cancer cachexia is a life endangering paraneoplastic syndrome characterized by loss of muscle mass and body weight that is accompanied by fatigue and generalized weakness [41]. According to National Cancer Institute, it is estimated that nearly one-third of deaths in cancer is due to cachexia [42]. The etiology of cachexia is multifactorial and is thought to be mediated, at least in part, by humoral factors that are secreted from or induced by the tumor which lead to an imbalance between the rates of protein synthesis and breakdown [43].

Colorectal cancer is the third leading cause of deaths due to cancer in United States and is characterized by neoplasms in the colon and rectum. Colorectal cancer originates from the epithelial cells and is most commonly due to a mutation in adenomatous polyposis coli (APC) gene [44]. The $Apc^{Min/+}$ mouse is a well-recognized model for use in colorectal cancer studies that exhibits a nonsense mutation at codon 850 in the *Apc* gene [3]. This mutation results in a truncated protein that predisposes the mice to intestinal neoplasms. Similar to humans, the $Apc^{Min/+}$ mouse exhibits intestinal neoplasms and severe muscle wasting with increasing tumor burden [45, 46].

Work to date has largely focused on understanding the mechanisms of skeletal muscle loss in cancer cachexia. Burc and colleagues, (1968) first demonstrated that existence of cardiac atrophy in cancer patients when they noted that cancer patients had smaller hearts and exhibited a diminution of the QRS complex both findings consistent with changes in cardiac function. Later work by Tessitore et al., (1993) examining male Wistar rats that had been injected with Yosidha ascites hepatoma cells found that heart mass was decreased by 21% by day 4 and to 46% by day 10 when compared to control animals [47]. The mechanism(s) responsible for the loss of cardiac mass in cancer cachexia have yet to be elucidated.

The objectives of this study were twofold: (i.) to determine if the $Apc^{Min/+}$ mouse exhibits cardiac atrophy with cachexia and (ii.) to examine the molecular signaling mechanism(s) that may

be activated in the *Apc*$^{Min/+}$ mouse heart during the cachectic response. We hypothesized that hearts from *Apc*$^{Min/+}$ mice would weigh less than their age matched control counterparts and that this decrease in cardiac mass would be associated with evidence of increased cardiac autophagy.

MATERIALS AND METHODS

Animals

All procedures were performed as outlined in the Guide for the Care and Use of Laboratory Animals as approved by the Council of the American Physiological Society and the Animal Use Review Board of Marshall University and University of South Carolina. Young (12 week, n=4) male C57BL/6 wild and *Apc*^{Min} mice and adult (20 week, n=4) male C57BL/6 and *Apc*^{Min} mice were purchased from Jackson Laboratories and maintained by Dr. James A. Carson (University of South Carolina). Animals were housed under a 12H: 12H dark-light cycle at 22° ± 2 °C. Mice were provided standard rodent chow (Harlan Teklad Rodent Diet, no. 8604) and water *ad libitum*. After acclimatization the mice were sacrificed according to the regulatory guidelines of University of South Carolina and the samples were sent to Marshall University in dry ice for analysis.

Materials

Anti- Akt (#9272), mTOR (#2972), p70s6k (#9202), S6 ribosomal protein (#2217), Nf-kB p65 (# 3034), Stat-3 (#9132), AMPK-α (#2532), Beclin1 (#3738), phosphorylated mTOR ^{Ser2448} (#2971), phosphorylated Akt ^{Thr308} (#9275), phosphorylated Akt ^{Ser473} (#9271), phosphorylated p70s6k $^{Thr421/Ser424}$ (#9204), phosphorylated S6 ribosomal protein $^{Ser235/236}$ (#4858), phosphorylated Nf-kB p65 ^{Ser536}, phosphorylated Stat-3 ^{Tyr705}, phosphorylated AMPK-α ^{Thr172} (#2535), Mouse IgG, and Rabbit IgG antibodies were purchased from Cell Signaling Technology (Beverly,

MA). HeLa Whole Cell Lysate (sc-2200) and L6 + IGF Lysate (sc-24727) were purchased from Santa Cruz Biotechnology (Santa Cruz, CA). Enhanced chemiluminescence (ECL) western blotting detection reagent was obtained from Amersham Biosciences (Piscataway, NJ). Restore western blot stripping buffer was purchased from Pierce (Rockford, IL). All other chemicals were purchased from Sigma Aldrich (St. Louis, MO) or Fisher Scientific (Hanover, IL).

Preparation of protein isolates and immunoblotting

Hearts were pulverized in liquid nitrogen using a mortar and pestle until a fine powder was obtained. After washing with ice cold PBS, pellets were lysed on ice for 15 minutes in T-PER (2 mL/1 g tissue weight) (Pierce, Rockford, IL) containing protease and phosphatase inhibitors and centrifuged for 10 minutes at 2000 X *g* to pellet particulate matter. This process was repeated twice and the supernatants used for protein concentration determination using the 660 nm assay (Pierce, Rockford, IL). Samples were diluted to a concentration of 2.5 μg/ μl in SDS loading buffer, boiled for 5 minutes at 95 °C, and 30 μg of protein were separated using 10% and 15% SDS-PAGE gels. Verification of transfer onto nitrocellulose membrane was determined by Ponceau staining and determination of equal loading between lanes and membranes was determined by using GAPDH as loading control. Protein detection was performed as outlined by the antibody manufacturer while immunoreactive bands were visualized with ECL (Amersham Biosciences). Exposure time was adjusted at all times to keep the integrated optical densities within a linear and non-saturated range, and band signal intensity was quantified by densitometry using a flatbed scanner (Epson Perfection 3200 Photo) and imaging software (AlphaEaseFC). Biotinylated ladder (Cell Signaling) was used as molecular mass standards and Hela Whole cell lysates along with L6 + IGF were included as positive controls. For direct comparisons between the concentration levels

of different signaling molecules, membranes were stripped and re-probed for different molecule with Restore western blot stripping buffer as detailed by the manufacturer (Pierce, Rockford, IL).

Statistical analysis

Results are presented as mean ± SEM. Data were analyzed by using the Sigma Stat 3.0 statistical program. Data were analyzed using a two-way ANOVA followed by the Student-Newman-Keuls post-hoc testing when appropriate. $P < 0.05$ was considered to be statistically significant.

RESULTS

Cancer cachexia and heart weight

Average body mass of the C57BL/6 mice was ~10% (25.8 ± 1.4 g vs. 23.2 ± 1.1 g; $P < 0.05$) and ~26% (27.3 ± 0.7 g vs. 20.2 ± 0.8 g; $P < 0.05$) greater than their $Apc^{Min/+}$ counterparts at 12- and 20-weeks, respectively (Table 1). Compared to 12 week C57BL/6 mice, heart muscle mass was ~8% less (120.4 ± 3.9 mg vs. 111.2 ± 3.6 mg; $P < 0.05$) in the 12 week $Apc^{Min/+}$ mice. Similarly, heart weights of 20-week old C57BL/6 mice were 6% greater than those of 20-week old $Apc^{Min/+}$ mice (115.8 ± 3.8 mg vs. 108.8 ± 5.9 mg; $P < 0.05$).

Cancer cachexia in the $Apc^{Min/+}$ mouse is associated with elevated cardiac Stat-3 and Nf-kB levels but not increased apoptosis.

The amount of total and phosphorylated Nf-kB p65 were significantly higher in 12- (20.9 ± 2.6%, 81.3 ± 3.7%) week and 20- (84.9 ± 10.6%, 171.2 ± 13.9%) week $Apc^{Min/+}$ mice ($P < 0.05$; Figure 1). Similarly, the amount of Stat-3 (28.1 ± 8.5%, 39.3 ± 10.6%) and phosphorylated Stat-3 (74.8 ± 20.0% and 37.1 ± 12.4%) were higher in 12- and 20-week $Apc^{Min/+}$ mice ($P < 0.05$; Figure

2). No evidence of increased caspase-3 or caspase-9 activation or cardiac apoptosis with cancer was observed (data not shown).

AMPKα phosphorylation is higher in the hearts of *Apc*$^{Min/+}$ mice

Compared to that observed in the control animals the amount of total and phosphorylated AMPK were 4.5 ± 1.1%, 4.2 ± 2.6% and 19.6 ± 5.2%, 22.5 ± 5.5 % higher in the 12- and 20-week old *Apc*$^{Min/+}$ mice, respectively ($P< 0.05$; Figure 3).

Akt signaling is activated in the hearts of *Apc*$^{Min/+}$ mice

To investigate the cancer cachexic effects on the total and phosphorylated amounts of Akt, mTOR, p70s6k, EIF4E, S6rp we performed SDS-PAGE and western blot analysis using antibodies which recognize both the unphosphorylated and phosphorylated forms of these molecules. There were no differences in Akt protein content among different groups (Figure 4). Compared to C57BL/6 controls, the phosphorylation of Akt (Ser308) was ~1.5 and ~2.5 fold higher in the 12- and 20-week *Apc*$^{Min/+}$ mice, respectively ($P< 0.05$; Figure 4). Similarly, with cancer the amount of phosphorylated Akt (Thr473) was ~ 0.75 and ~1.25 fold higher in 12- and 20-week *Apc*$^{Min/+}$ mice, respectively ($P< 0.05$; Figure 4). The expression of mTOR was significantly higher in 12 week and 20 week *Apc*$^{Min/+}$ mice by 38.5 ± 8.1% and 17.1 ± 7.6% compared to age matched C57BL/6 mice controls ($P< 0.05$; Figure 5). The total level of p70s6k was 23.2 ± 2.4% lower in 12 week *Apc*$^{Min/+}$ mice and 19.3 ± 3.5% higher in 20 week *Apc*$^{Min/+}$ mice compared to that observed in age-matched control animals ($P< 0.05$; Figure 6). Immunoblot analysis using phospho-specific antibodies indicated that the total phosphorylation level of mTOR (Ser2448) and p70s6k (Thr421/Ser424) were 23.2 ± 13.2%, 44.0 ± 16.4% and 36.5 ± 9.4%, 104.9 ± 24.8% higher, respectively in 12- week and 20-week *Apc*$^{Min/+}$ mice compared to

age-matched controls ($P< 0.05$; Figures 5, 6). The levels of S6rp were decreased in both cachexic groups compared to their controls while the phosphorylation of S6rp was decreased in 20- week $Apc^{Min/+}$ mice ($P< 0.05$; Figure 7). Phosphorylated levels of Bad at Ser136 were significantly increased in both 12 week and 20 week $Apc^{Min/+}$ mice by approximately 100% and 74%, respectively ($P< 0.05$; Figure 8).

Expression of autophagy regulating proteins but not calpain expression or protein ubiquitination is increased in cancer-induced cachexic hearts

It is thought that muscle utilizes three different proteolytic pathways to regulate muscle protein breakdown: calcium-dependent calpains, the ubiquitin-proteasome system and autophagy [1]. Compared to that observed in the control animals, no evidence of calpain activation (data not shown) or increased ubiquitination was observed in the $Apc^{Min/+}$ mice (data not shown). Conversely, immunoblot analysis revealed that the expression of the autophagy regulator Beclin1 was 4.7 ± 3.3% and 9.5 ± 3.0% higher in the 12- and 20-week old $Apc^{Min/+}$ mice, respectively ($P< 0.05$; Figure 9).

DISCUSSION

Cancer cachexia is thought to be the cause of about 30% of all cancer-related deaths. How cancer may affect cardiac mass is only just now beginning to be investigated. Although cardiac mass in the *Apc*$^{Min/+}$mouse colorectal cancer model was decreased at both 12- and 20-weeks when compared to age-matched control animals there was not a significant decrease in the heart to body weight ratio in 12-weeks *Apc*$^{Min/+}$mouse (Table 1). These data suggest that cardiac atrophy does not occur to a significant extent in the *Apc*$^{Min/+}$ mouse. This finding is interesting given that the degree of gastrocnemius (-41%) and soleus (-26%) muscle atrophy in the 20-week old *Apc*$^{Min/+}$ mouse is quite apparent [48]. Taken together, these data are consistent with the possibility that different muscle types exhibit different susceptibility to atrophy. This finding is not new. It is well established that the slow twitch soleus muscle is more sensitive to unloading-induced atrophy than the fast twitch plantaris muscle [49]. Why different muscle types might experience different degrees of muscle loss following exposure to atrophic stimuli is not well understood.

It appears that the effects of colorectal cancer on cardiac mass may be different from that observed in other cancer models. For example, using the Yoshida tumor implant model Costelli and Melloni demonstrated significant loss of cardiac mass within six to ten days of implant [50]. More recently, Cosper and Leinwand using colon-26 adenocarcinoma implants showed that cardiac mass was decreased by approximately 8% and 21 % at 15 and 27 days post implantation, respectively [1]. The reason(s) why different cancer models may affect the regulation of heart mass differently is not clear but could be related to the amount or type of humoral factors released by the tumor. For example, the muscle wasting seen in the Yoshida heptatoma ascites model is generally considered to be the result of elevations in TNF-alpha

while muscle loss in the colon-26 adenocarcinoma tumor implant model has been shown to be associated with increases in the amount of IL-1, IL-6, IL-12 and TNF-alpha [51-53].

In the case of the *Apc*$^{Min/+}$ mouse model, it is generally thought that the atrophy induced in this model is due to an elevation in serum IL-6 levels [41, 46, 48]. How IL-6 may affect cardiac structure or function is poorly understood. Recent data suggests that burn injury and sepsis are associated with cardiac inflammation, increased apoptosis and depressed contractile function [54, 55]. Similar to the *Apc*$^{Min/+}$ mouse model, these aforementioned conditions are characterized by sustained increases in IL-6 levels. Other work has demonstrated that IL-6 can activate AMPK [56]. In the present study we found evidence of increased NF-kB and Stat-3 activation which are consistent with the possibility of increased cardiac inflammation (Figures 1, 2). In addition, we also found increases in pAMPK levels (Figure 3). Whether the increases in pAMPK we observe are due to elevations in IL-6, changes in nutrient uptake secondary to colon tumor load, or some combination of the two is currently unclear.

In contrast to that observed in the septic and burn models we did not find any evidence of increased cardiac apoptosis (data not shown). This finding is similar to what others have seen upon investigating cardiac atrophy in the C-26 adenocarcinoma tumor implant model (Cosper and Leinwand). Given that elevations in IL-6 levels can cause cardiac apoptosis, our findings, along with those of Cosper and Leinwand, were quite surprising initially. To try to ascertain the potential mechanism(s) behind this finding we examined the phosphorylation status of Akt. The Akt is a serine / threonine kinase which is involved in the regulation of cell metabolism and cell death [57]. With cancer, we found an elevation in Akt phosphorylation at both Thr 308 and Ser 473 (Figure 4) which is consistent with Akt activation. Given that Akt activation is strongly anti-apoptotic, we interpret these data to suggest that this is a compensatory response that is initiated to stave off the possibility of IL-6 induced cardiomyocyte apoptosis. In addition to

Akt, the activation of mTOR has also been shown to inhibit cellular death [58]. Similar to our findings for Akt, we also found significant elevations in mTOR phosphorylation with cancer. To confirm these findings, we next examined the phosphorylation of p70S6k which is a downstream substrate of mTOR. As expected, we found elevations in the activation (phosphorylation) of p70S6k and its downstream effector Bad (Figures 4, 8). Like Akt, Bad is intimately involved in regulating the transition between cellular life and death. In its unphosphorylated form Bad is strongly apoptotic [59, 60]. Conversely, when phosphorylated, the apoptotic activity of Bad is inhibited and cell death is prohibited. We suspect that the elevations in the phosphorylation of Akt, mTOR, p70S6k and Bad that we observe in the APC min mouse are an attempt by the cardiomyocyte to minimize cardiac apoptosis and preserve cardiac function. In an effort to further investigate this possibility we next examined the phosphorylation of the downstream effector of p70s6k, S6rp. In 20 weeks $Apc^{Min/+}$ mice we found activation of Akt and mTOR and p70s6k (Thr421/Ser424), but a decrease in activated S6rp (Figure 7). These data suggest that the p70S6k activation we observe is most likely directed towards anti-apoptotic signaling and not for the purpose of increasing protein synthesis.

It is thought that muscle utilizes three different proteolytic pathways to regulate muscle protein breakdown: Ca-dependent calpains, the ubiquitin-proteasome system and autophagy [1]. Autophagy is a mechanism for cell protection in which intracellular substances are degraded and the subsequent products recycled again. The breakdown of proteins that are not used in cellular metabolism leads to production of amino acids. On the basis of recent data suggesting that cancer cachexia is associated with increased autophagy [1] and other findings demonstrating that increased AMPK phosphorylation can stimulate this process [61] we next examined the regulation of beclin1. Our data demonstrated that cancer was associated with

beclin1 levels (Figure 9). These data suggest that changes in cardiac mass in the *Apc*$^{Min/+}$ mouse may be associated with autophagy.

Taken together, our data suggest that cachexia in the *Apc*$^{Min/+}$ mouse model is associated with inflammation but not cardiac atrophy. Given the absence of changes in cardiac mass, cardiac apoptosis and protein ubiquitination we suspect that the activation of Akt, mTOR and p70s6k observed in the present study are more related to efforts directed at maintaining cell survival rather than increasing protein synthesis (Figure 10). Future studies designed to directly test this possibility will no doubt be useful in better understanding the effects of colorectal cancer on the heart.

APPENDIX

TABLES AND FIGURES

TABLE 1

Animals	**Heart Weight (mg)**	**Body Weight (gm)**	**Hrt. / B.W. Ratio**
12 week BL6 mice	120.4 ± 3.9	25.7 ± 1.4	4.7 ± 0.12
12 week *Apc*$^{Min/+}$ mice	111.2 ± 3.6*	23.1 ± 1.1*	4.8 ± 0.3
20 week BL6 mice	115.8 ± 3.8	27.3 ± 0.3	4.2 ± 0.2
20 week *Apc*$^{Min/+}$ mice	108.8 ± 5.9*	20.1 ± 0.8*	5.4 ± 0.5*

Figure 1

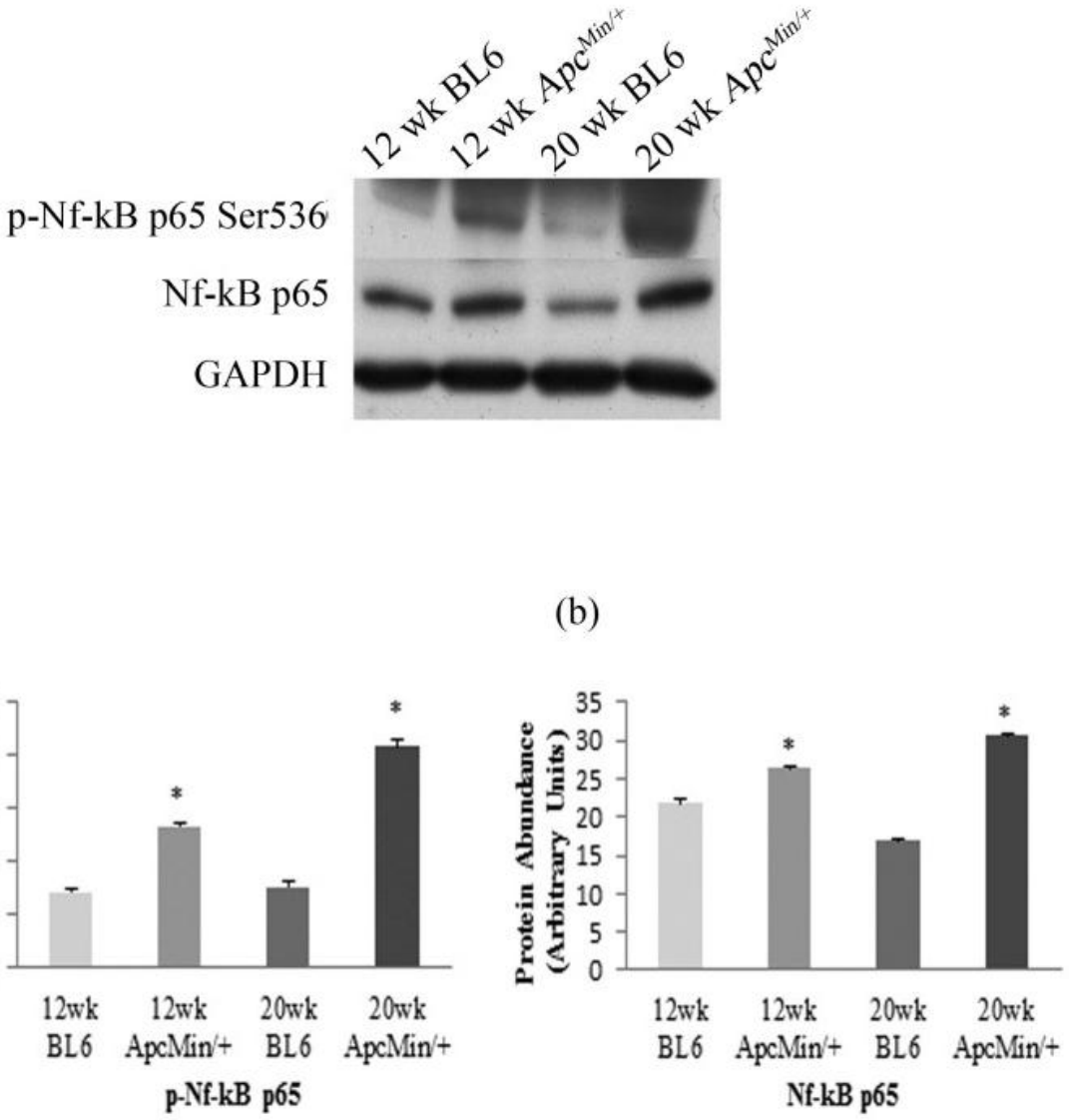
12 wk BL6
12 wk ApcMin/+
20 wk BL6
20 wk ApcMin/+
p-Nf-kB p65 Ser536
Nf-kB p65
GAPDH
(a)
Protein Abundance (Arbitrary Units)
50
40
30
20
10
0
*
*
12wk BL6
12wk ApcMin/+
20wk BL6
20wk ApcMin/+
p-Nf-kB p65
(b)
Protein Abundance (Arbitrary Units)
35
30
25
20
15
10
5
0
*
*
12wk BL6
12wk ApcMin/+
20wk BL6
20wk ApcMin/+
Nf-kB p65

Figure 2

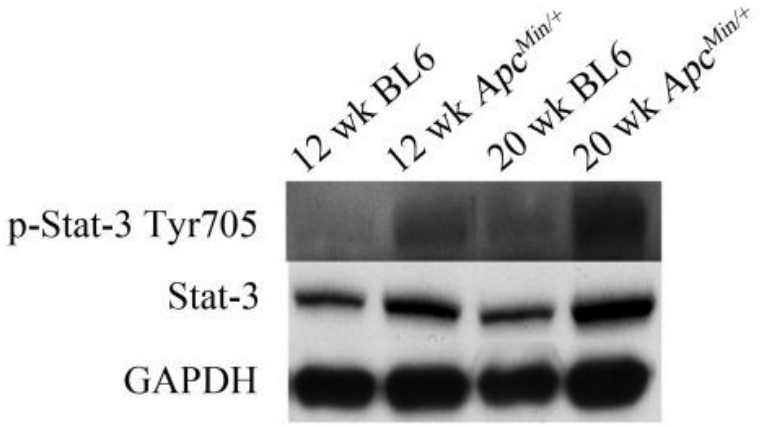
12 wk BL6
12 wk ApcMin/+
20 wk BL6
20 wk ApcMin/+
p-Stat-3 Tyr705
Stat-3
GAPDH

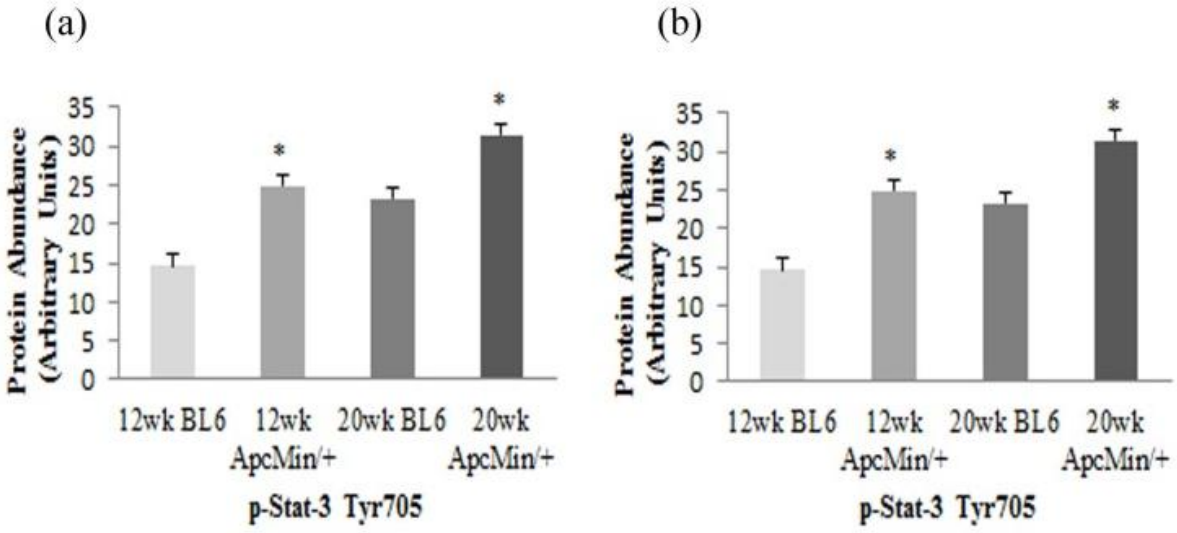
(a)
(b)
Protein Abundance (Arbitrary Units)
35
30
25
20
15
10
5
0
*
12wk BL6
12wk ApcMin/+
20wk BL6
20wk ApcMin/+
p-Stat-3 Tyr705

Figure 3

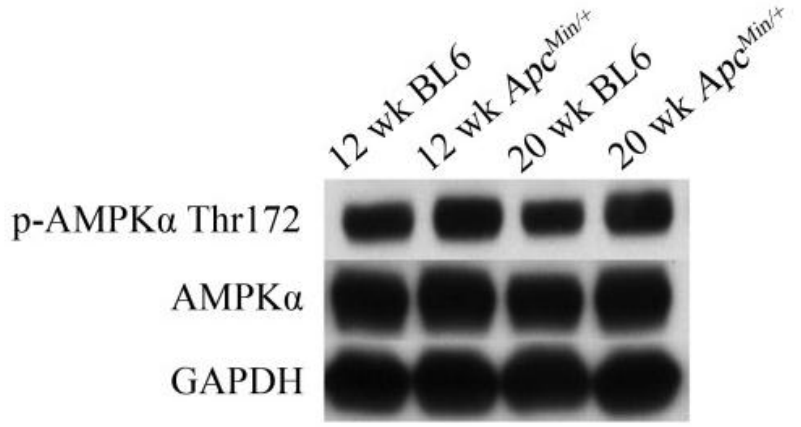
12 wk BL6
12 wk ApcMin/+
20 wk BL6
20 wk ApcMin/+
p-AMPKα Thr172
AMPKα
GAPDH

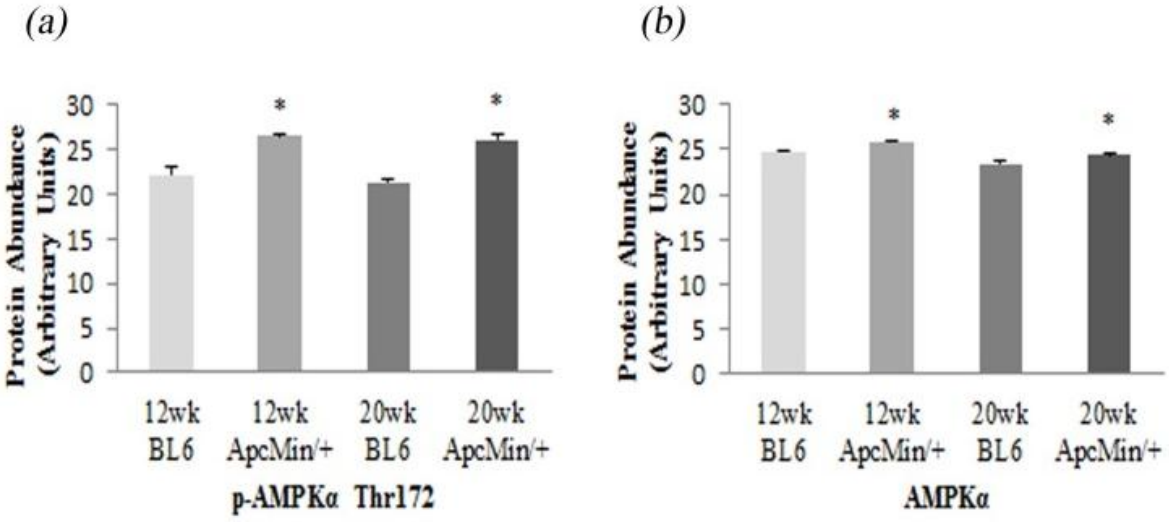
(a)
(b)
Protein Abundance (Arbitrary Units)
30
25
20
15
10
5
0
*
*
12wk BL6
12wk ApcMin/+
20wk BL6
20wk ApcMin/+
p-AMPKα Thr172
AMPKα

Figure 4

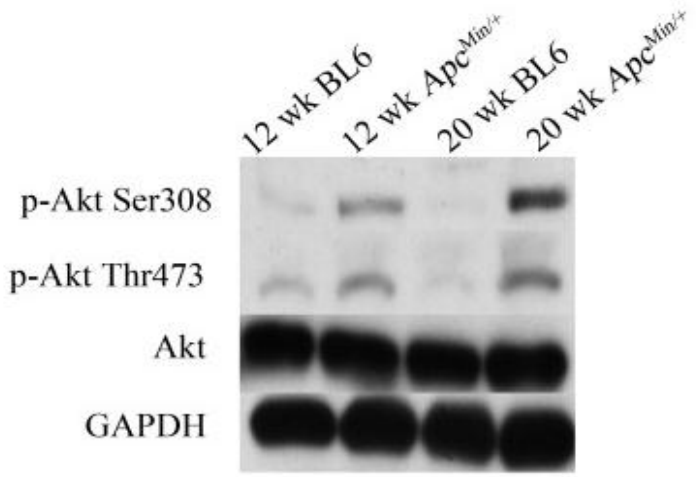
12 wk BL6
12 wk ApcMin/+
20 wk BL6
20 wk ApcMin/+
p-Akt Ser308
p-Akt Thr473
Akt
GAPDH

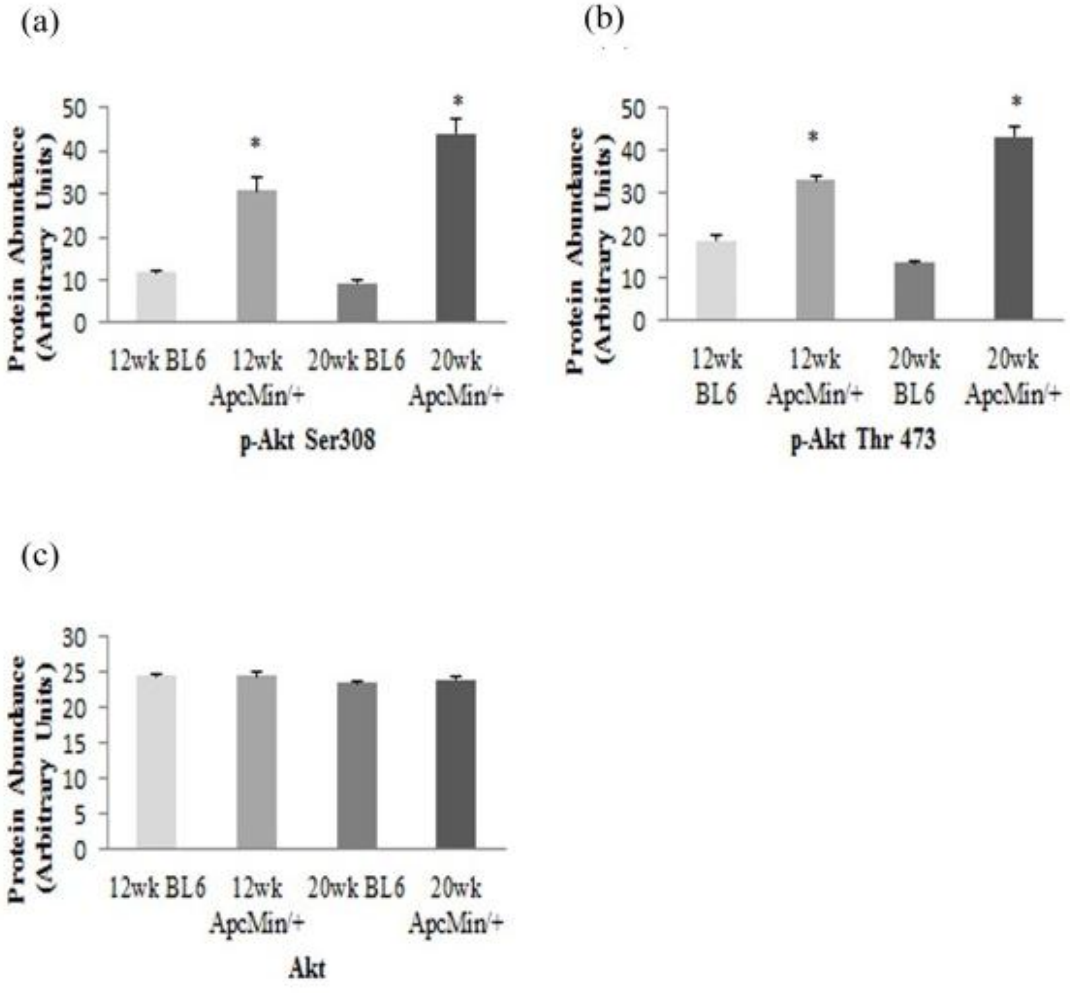
(a)
Protein Abundance (Arbitrary Units)
50
40
30
20
10
0
*
*
12wk BL6
12wk ApcMin/+
20wk BL6
20wk ApcMin/+
p-Akt Ser308
(b)
Protein Abundance (Arbitrary Units)
50
40
30
20
10
0
*
*
12wk BL6
12wk ApcMin/+
20wk BL6
20wk ApcMin/+
p-Akt Thr 473
(c)
Protein Abundance (Arbitrary Units)
30
25
20
15
10
5
0
12wk BL6
12wk ApcMin/+
20wk BL6
20wk ApcMin/+
Akt

Figure 5

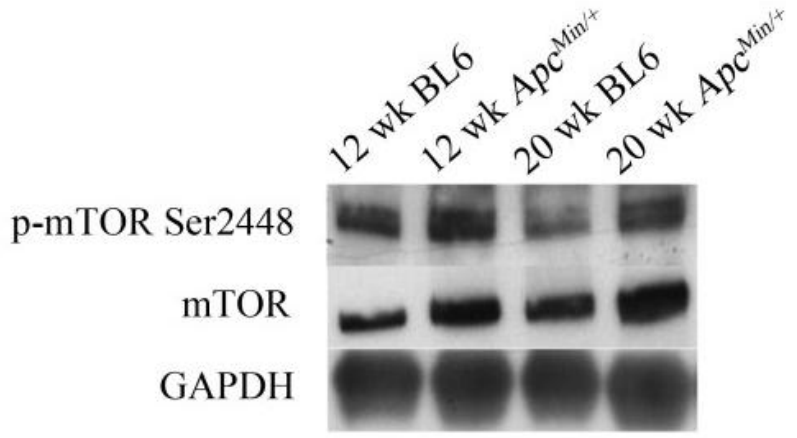
12 wk BL6
12 wk ApcMin/+
20 wk BL6
20 wk ApcMin/+
p-mTOR Ser2448
mTOR
GAPDH

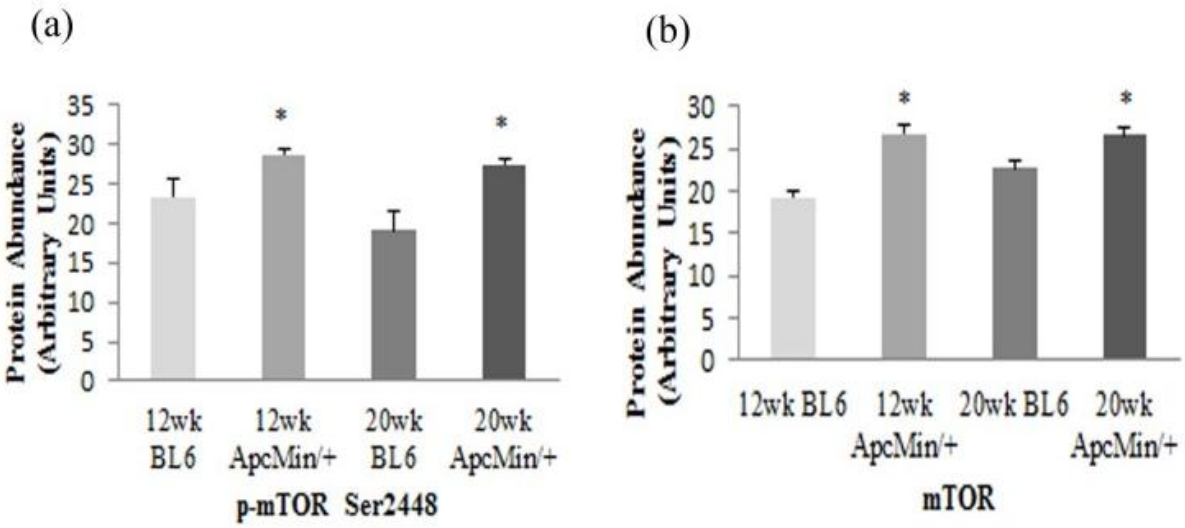
(a)
Protein Abundance (Arbitrary Units)
35
30
25
20
15
10
5
0
*
*
12wk BL6
12wk ApcMin/+
20wk BL6
20wk ApcMin/+
p-mTOR Ser2448
(b)
Protein Abundance (Arbitrary Units)
30
25
20
15
10
5
0
*
*
12wk BL6
12wk ApcMin/+
20wk BL6
20wk ApcMin/+
mTOR

Figure 6

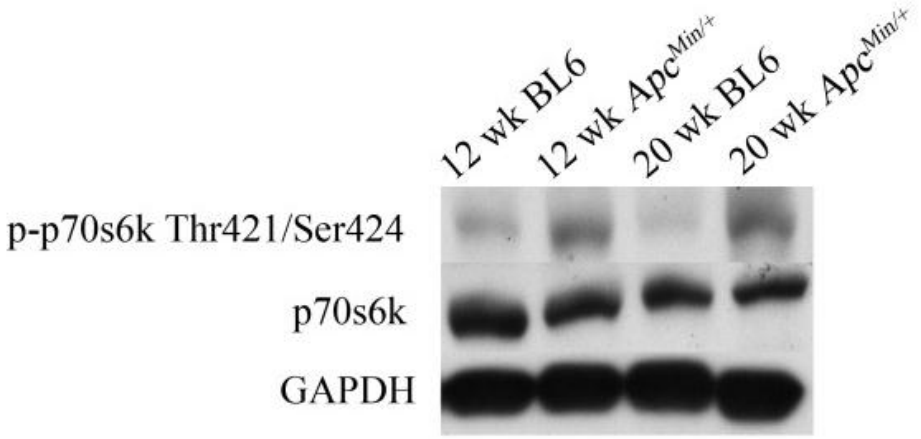
12 wk BL6
12 wk ApcMin/+
20 wk BL6
20 wk ApcMin/+
p-p70s6k Thr421/Ser424
p70s6k
GAPDH

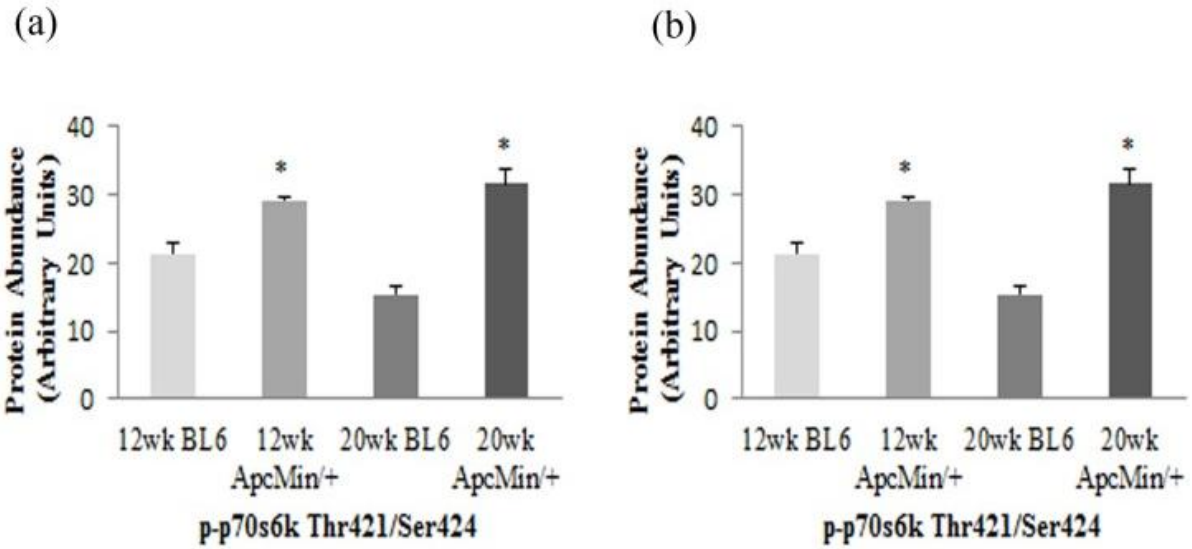
(a)
(b)
Protein Abundance (Arbitrary Units)
40
30
20
10
0
*
*
12wk BL6
12wk ApcMin/+
20wk BL6
20wk ApcMin/+
p-p70s6k Thr421/Ser424

Figure 7

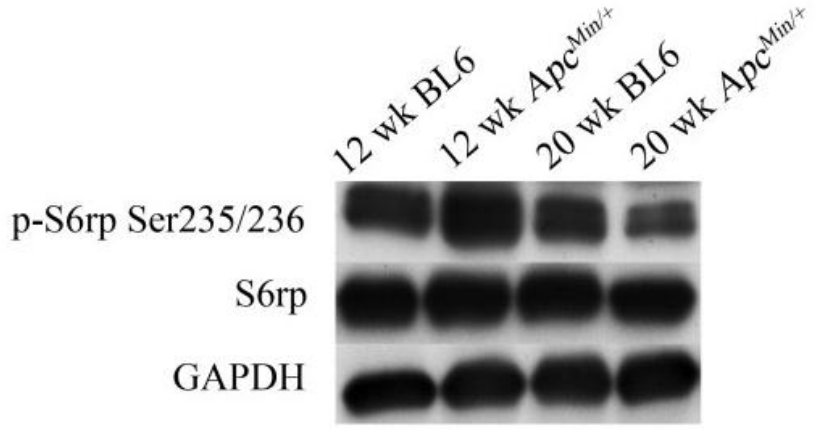
12 wk BL6
12 wk ApcMin/+
20 wk BL6
20 wk ApcMin/+
p-S6rp Ser235/236
S6rp
GAPDH

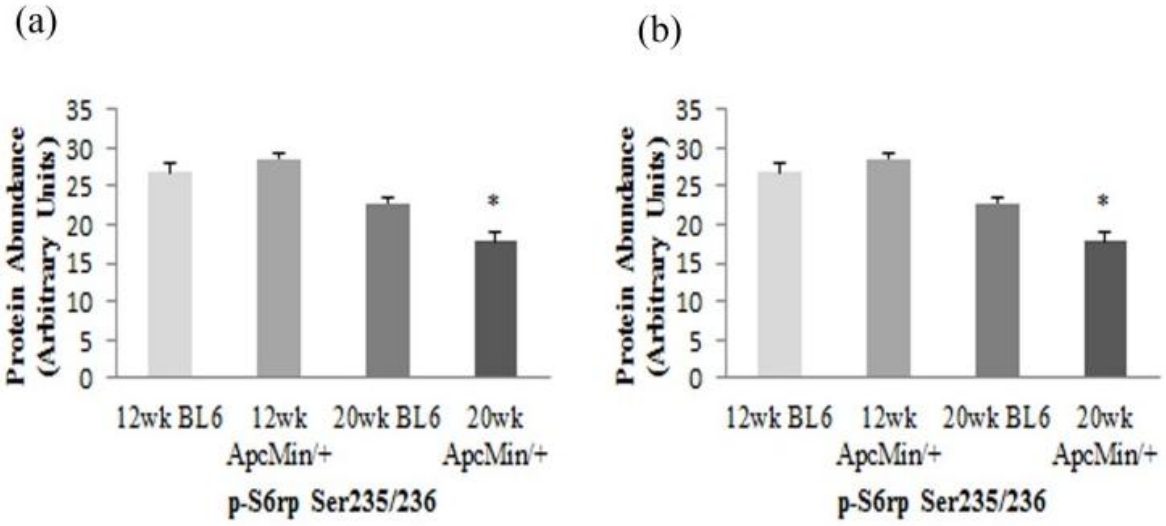
(a)
(b)
Protein Abundance (Arbitrary Units)
35
30
25
20
15
10
5
0
*
12wk BL6
12wk ApcMin/+
20wk BL6
20wk ApcMin/+
p-S6rp Ser235/236

Figure 8

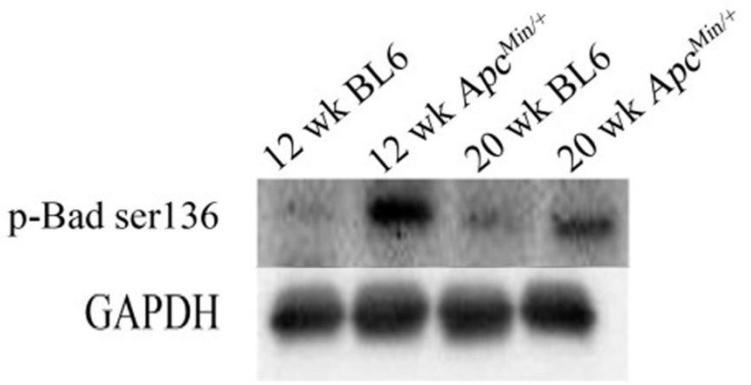
12 wk BL6
12 wk ApcMin/+
20 wk BL6
20 wk ApcMin/+
p-Bad ser136
GAPDH

(a)

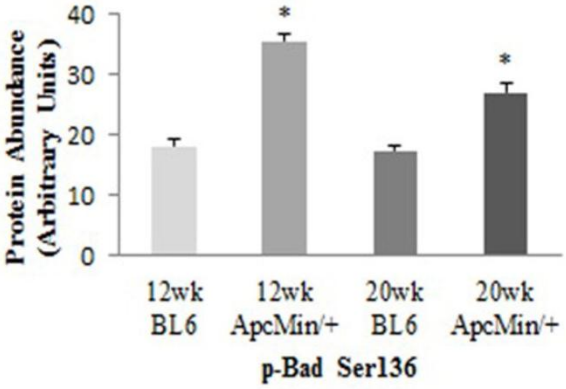
Protein Abundance (Arbitrary Units)
40
30
20
10
0
*
*
12wk BL6
12wk ApcMin/+
20wk BL6
20wk ApcMin/+
p-Bad Ser136

Figure 9

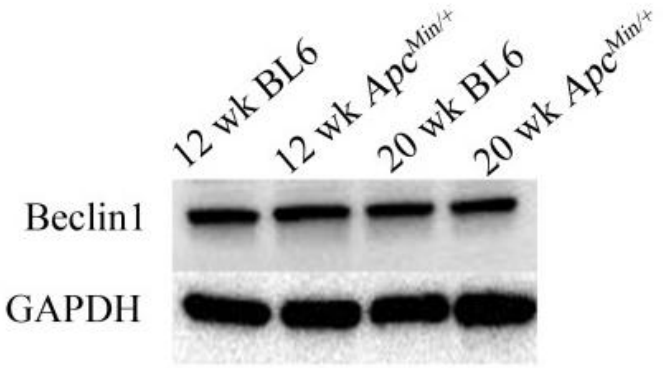
12 wk BL6
12 wk ApcMin/+
20 wk BL6
20 wk ApcMin/+
Beclin1
GAPDH

(a)

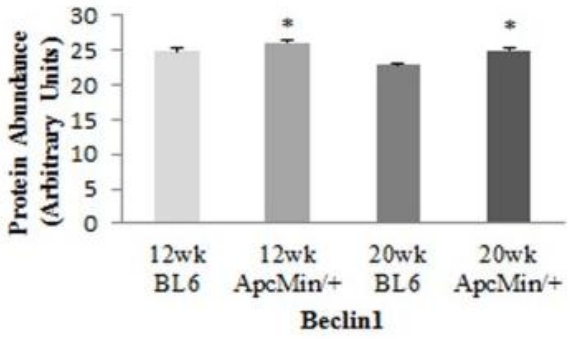
Protein Abundance (Arbitrary Units)
30
25
20
15
10
5
0
*
*
12wk BL6
12wk ApcMin/+
20wk BL6
20wk ApcMin/+
Beclin1

Figure 10

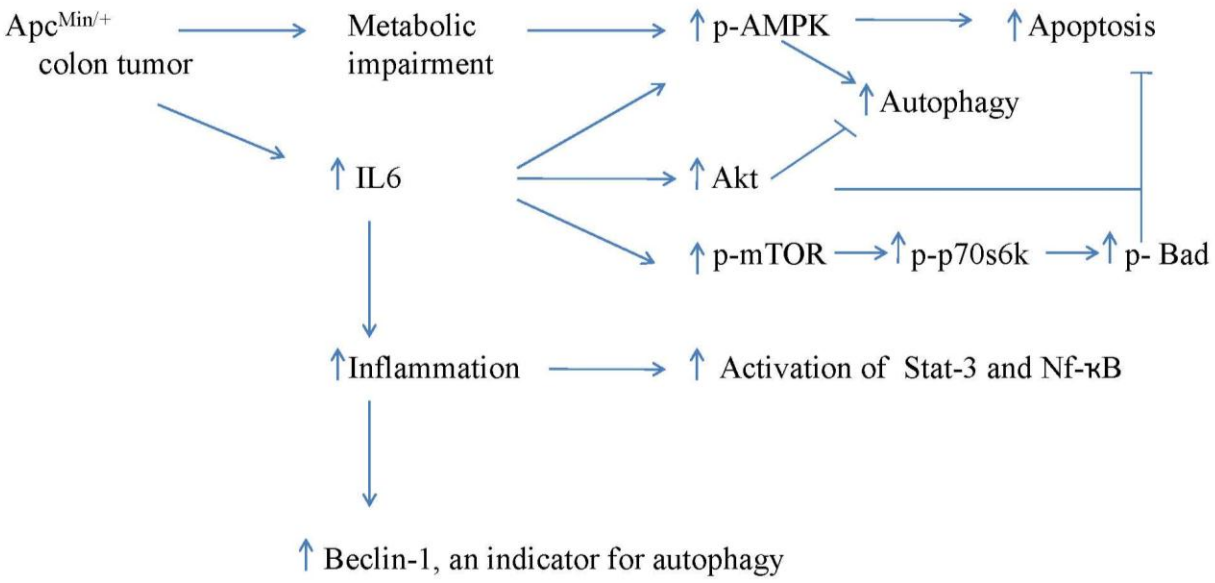
Apc^Min/+ colon tumor
Metabolic impairment
↑ p-AMPK
↑ Apoptosis
↑ Autophagy
↑ IL6
↑ Akt
↑ p-mTOR
↑ p-p70s6k
↑ p- Bad
↑ Inflammation
↑ Activation of Stat-3 and Nf-κB
↑ Beclin-1, an indicator for autophagy

FIGURE LEGENDS

Figure 1. Total and phosphorylated levels of Nf-kB p65 is altered in colorectal cancer induced cachexia. Total and phosphorylated levels of Nf-kB p65 in BL6 and *Apc*$^{Min/+}$ mice at 12- and 20-weeks. Results are expressed as arbitrary units for comparison. An asterisk (*) indicates significant differences in *Apc*$^{Min/+}$ mice from the BL6 age matched controls ($P< 0.05$).

Figure 2. Total and phosphorylated levels of Stat-3 are altered in colorectal cancer induced cachexia. Total and phosphorylated levels of Stat-3 at Tyr 705 in BL6 and *Apc*$^{Min/+}$ mice at 12- and 20-weeks. Results are expressed as arbitrary units for comparison. An asterisk (*) indicates significant differences in *Apc*$^{Min/+}$ mice from the BL6 age matched controls ($P< 0.05$).

Figure 3. Total and phosphorylated levels of AMPKα are altered in colorectal cancer induced cachexia. Total and phosphorylated levels of AMPKα at Thr172 in BL6 and *Apc*$^{Min/+}$ mice at 12- and 20-weeks. Results are expressed as arbitrary units for comparison. An asterisk (*) indicates significant differences in *Apc*$^{Min/+}$ mice from the BL6 age matched controls ($P< 0.05$).

Figure 4. Cancer cachexia is associated with activation of cardiac Akt. Heart muscles from BL6 and *Apc*$^{Min/+}$ were analyzed by Western blot analysis for cachexia-related changes in total and phosphorylated levels of Akt at Ser 308 and Thr473. Results are expressed as arbitrary units for comparison. An asterisk (*) indicates significant differences in *Apc*$^{Min/+}$ mice from the BL6 age matched controls ($P< 0.05$).

Figure 5. Cancer cachexia induced changes in total and phosphorylated levels of mTOR. Total and phosphorylated levels of mTOR at Ser2448 were analyzed by immunoblotting. Results are expressed as arbitrary units for comparison. An asterisk (*) indicates significant differences in $Apc^{Min/+}$ mice from the BL6 age matched controls ($P< 0.05$).

Figure 6. Total and phosphorylated levels of p70s6k are altered in cancer cachexia. Immunoblot analysis for total and phosphorylated p70s6k at Thr421/Ser424 in BL6 and $Apc^{Min/+}$ mice of 12 and 20 weeks. Results are expressed as arbitrary units for comparison. An asterisk (*) indicates significant differences in $Apc^{Min/+}$ mice from the BL6 age matched controls ($P< 0.05$).

Figure 7. Total and phosphorylated levels of S6 ribosomal protein is altered in cancer cachexia. Total and phosphorylated levels of S6RP at Ser235/236 in BL6 and $Apc^{Min/+}$ mice at 12- and 20-weeks. Results are expressed as arbitrary units for comparison. An asterisk (*) indicates significant differences in $Apc^{Min/+}$ mice from the BL6 age matched controls ($P< 0.05$).

Figure 8. Phosphorylated levels of Bad are altered with cancer induced cachexia. Phosphorylated levels of Bad at Ser136 in BL6 and $Apc^{Min/+}$ mice at 12- and 20-weeks. Results are expressed as arbitrary units for comparison. An asterisk (*) indicates significant differences in $Apc^{Min/+}$ mice from the BL6 age matched controls ($P< 0.05$).

Figure 9. Alterations in autophagy indicator molecule Beclin1 is associated with cancer cachexia. Total levels of Beclin1 in BL6 and $Apc^{Min/+}$ mice at 12- and 20-weeks of age. Results are expressed as arbitrary units for comparison. An asterisk (*) indicates significant differences in $Apc^{Min/+}$ mice from the BL6 age matched controls ($P< 0.05$).

Figure 10. Schematic representation of different pathways involved in cancer induced cardiac cachexia in *Apc*$^{Min/+}$ mice.

CHAPTER 4

Conclusions

1. The amount of total and phosphorylated AMPK, and Akt/mTOR are altered in hearts of $Apc^{Min/+}$ mice.
2. There is no change in overall ubiquitination in $Apc^{Min/+}$ compared to age matched BL6 controls. However there is an increase in autophagy in $Apc^{Min/+}$ as indicated by expression of beclin1.
3. Total and phosphorylated levels of proteins in Nf-kB and Stat-3 are increased in hearts of mice with cancer cachexia.
4. The degree of cardiac atrophy seen in the $Apc^{Min/+}$ mouse cancer model is less than that observed in other rapidly growing tumor models. Given the interaction between different signaling pathways, we suspect that cardiac mass is maintained by increased Akt/mTOR pathway signaling which acts to counterbalance the increases in AMPK and beclin1 activation.

Future Directions

Future directions based on this study should be aimed at the effects of cancer cachexia on cardiac function and its structure. How cancer cachexia effects cardiac function remains unclear and needs to be investigated in order to go for therapeutic intervention. Previous studies have shown that mice injected with colon-26 adenocarcinoma exhibited a significantly reduced fractional shortening compared to their controls. The same researchers found that mRNA and protein levels for MHC were altered with a decrease in MHCalpha (adult isoform) and an increase in MHCbeta (fetal isoform) indicating reactivation of the fetal gene expression [62]. A similar study conducted by a different group showed that left ventricular systolic diameter was increased

and diastolic posterior wall thickness was decreased significantly in tumor-bearing mice indicating a severe cardiac dysfunction [63]. However it is interesting to find out if similar changes would be seen in *Apc*$^{Min/+}$ mice model of colon cancer.

It is also worthwhile to see if the changes associated with cardiac dysfunction correlate with altered cardiac structure and any evidence of marked fibrosis. Tian.M (2010) showed that mice injected with colon-26 adenocarcinoma exhibited increased fibrosis and transmission electron microscopy revealed disrupted myocardial ultrastructure [62]. A more recent study conducted on both male and female mice bearing tumors showed that there is a marked increase in fibrosis by 50% and 65% compared to their controls along with myocellular disarray. The same group also showed that cardiac atrophy in this case was associated with a decrease in myocyte size but not an increase in cell death [1]. It is however unknown if similar changes exist in *Apc*$^{Min/+}$ mice with colon cancer.

Cardiac muscle exhibits two isoforms of myosin (alpha and beta). While alpha is the predominant form in the healthy heart, a switch to the beta form occurs in a failing heart. The significant difference between the two isoforms is that alpha isoform can contract quickly utilizing more ATP while the beta isoform contracts slowly and strongly utilizing lesser ATP. It is thought that the increased workload or decreased activity of the glycolytic pathway might induce the change in isoform expression in order to maintain its normal function.[64, 65]. Previous work has demonstrated that diabetes, cardiomyopathy and exposure to hypoxia result in changes in cardiac myosin heavy chain expression [66-68] . Recent studies have reported a change in isoform switch in cachexic models which are injected with either with C-26 adenocarcinoma or Yoshida AH-130 ascites hepatoma cells [1]. Whether a similar finding may exist in the *Apc*$^{Min/+}$ mouse has, to our knowledge, not been investigated.

References

1. Cosper, P.F. and L.A. Leinwand, *Cancer causes cardiac atrophy and autophagy in a sexually dimorphic manner.* Cancer Res, 2011. **71**(5): p. 1710-20.
2. Vanchieri, C., *Cachexia in cancer: is it treatable at the molecular level?* J Natl Cancer Inst, 2010. **102**(22): p. 1694-7.
3. Moser, A.R., H.C. Pitot, and W.F. Dove, *A dominant mutation that predisposes to multiple intestinal neoplasia in the mouse.* Science, 1990. **247**(4940): p. 322-4.
4. Nieder, C., et al., *Comorbidity, use of common medications, and risk of early death in patients with localized or locally advanced prostate cancer.* ScientificWorldJournal, 2011. **11**: p. 1178-86.
5. Dhalla, N.S., et al., *Subcellular remodelling may induce cardiac dysfunction in congestive heart failure.* Cardiovasc Res, 2009. **81**(3): p. 429-38.
6. Mariotto, A.B., et al., *Projections of the cost of cancer care in the United States: 2010-2020.* J Natl Cancer Inst, 2011. **103**(2): p. 117-28.
7. Paul, P.K., et al., *Targeted ablation of TRAF6 inhibits skeletal muscle wasting in mice.* J Cell Biol, 2010. **191**(7): p. 1395-411.
8. Alexander, A. and C.L. Walker, *The role of LKB1 and AMPK in cellular responses to stress and damage.* FEBS Lett, 2011. **585**(7): p. 952-7.
9. Hardie, D.G., *AMP-activated protein kinase: a cellular energy sensor with a key role in metabolic disorders and in cancer.* Biochem Soc Trans, 2011. **39**(1): p. 1-13.
10. Comstock, E.G., *Guide to management of drug overdose.* Clin Toxicol, 1975. **8**(4): p. 475-82.
11. Shackelford, D.B. and R.J. Shaw, *The LKB1-AMPK pathway: metabolism and growth control in tumour suppression.* Nat Rev Cancer, 2009. **9**(8): p. 563-75.
12. Herrero-Martin, G., et al., *TAK1 activates AMPK-dependent cytoprotective autophagy in TRAIL-treated epithelial cells.* EMBO J, 2009. **28**(6): p. 677-85.
13. Gormand, A., et al., *Regulation of AMP-activated protein kinase by LKB1 and CaMKK in adipocytes.* J Cell Biochem, 2011. **112**(5): p. 1364-75.
14. McGaffin, K.R., et al., *Cardiac-specific leptin receptor deletion exacerbates ischaemic heart failure in mice.* Cardiovasc Res, 2011. **89**(1): p. 60-71.
15. Penna, F., et al., *Muscle atrophy in experimental cancer cachexia: is the IGF-1 signaling pathway involved?* Int J Cancer, 2010. **127**(7): p. 1706-17.
16. Suryawan, A., et al., *Leucine stimulates protein synthesis in skeletal muscle of neonatal pigs by enhancing mTORC1 activation.* Am J Physiol Endocrinol Metab, 2008. **295**(4): p. E868-75.
17. Hardie, D.G., *AMPK and Raptor: matching cell growth to energy supply.* Mol Cell, 2008. **30**(3): p. 263-5.
18. Baar, K. and K. Esser, *Phosphorylation of p70(S6k) correlates with increased skeletal muscle mass following resistance exercise.* Am J Physiol, 1999. **276**(1 Pt 1): p. C120-7.
19. Suryawan, A., et al., *Leucine acts as a nutrient signal to stimulate protein synthesis in neonatal pigs.* J Anim Sci, 2010.
20. Wang, X., et al., *Inhibition of mammalian target of rapamycin induces phosphatidylinositol 3-kinase-dependent and Mnk-mediated eukaryotic translation initiation factor 4E phosphorylation.* Mol Cell Biol, 2007. **27**(21): p. 7405-13.
21. Martelli, A.M., et al., *Targeting the Phosphatidylinositol 3-Kinase/Akt/Mammalian Target of Rapamycin Signaling Network in Cancer Stem Cells.* Curr Med Chem, 2011.
22. Zhang, X., et al., *Akt, FoxO and regulation of apoptosis.* Biochim Biophys Acta, 2011.
23. *Abstracts of the 2nd International Symposium on the Molecular Biology of Breast Cancer, Lillehammer, Norway, 12 - 16 March 2000.* Breast Cancer Res, 2000. **2 Suppl 1**: p. P1 01-S36.

24. Ming, X.F., et al., *Rho GTPase/Rho kinase negatively regulates endothelial nitric oxide synthase phosphorylation through the inhibition of protein kinase B/Akt in human endothelial cells.* Mol Cell Biol, 2002. **22**(24): p. 8467-77.
25. Danial, N.N., *BAD: undertaker by night, candyman by day.* Oncogene, 2008. **27 Suppl 1**: p. S53-70.
26. Asp, M.L., et al., *Evidence for the contribution of insulin resistance to the development of cachexia in tumor-bearing mice.* Int J Cancer, 2010. **126**(3): p. 756-63.
27. Schmitt, T.L., et al., *Activity of the Akt-dependent anabolic and catabolic pathways in muscle and liver samples in cancer-related cachexia.* J Mol Med, 2007. **85**(6): p. 647-54.
28. Thorburn, A., *Apoptosis and autophagy: regulatory connections between two supposedly different processes.* Apoptosis, 2008. **13**(1): p. 1-9.
29. Kanamori, H., et al., *The role of autophagy emerging in postinfarction cardiac remodelling.* Cardiovasc Res, 2011.
30. Shang, L. and X. Wang, *AMPK and mTOR coordinate the regulation of Ulk1 and mammalian autophagy initiation.* Autophagy, 2011. **7**(8).
31. Kim, J., et al., *AMPK and mTOR regulate autophagy through direct phosphorylation of Ulk1.* Nat Cell Biol, 2011. **13**(2): p. 132-41.
32. Burlacu, A., *Regulation of apoptosis by Bcl-2 family proteins.* J Cell Mol Med, 2003. **7**(3): p. 249-57.
33. Youle, R.J. and A. Strasser, *The BCL-2 protein family: opposing activities that mediate cell death.* Nat Rev Mol Cell Biol, 2008. **9**(1): p. 47-59.
34. Liu, Y., et al., *Proline oxidase activates both intrinsic and extrinsic pathways for apoptosis: the role of ROS/superoxides, NFAT and MEK/ERK signaling.* Oncogene, 2006. **25**(41): p. 5640-7.
35. Bajaj, G. and R.K. Sharma, *TNF-alpha-mediated cardiomyocyte apoptosis involves caspase-12 and calpain.* Biochem Biophys Res Commun, 2006. **345**(4): p. 1558-64.
36. Kantari, C. and H. Walczak, *Caspase-8 and bid: caught in the act between death receptors and mitochondria.* Biochim Biophys Acta, 2011. **1813**(4): p. 558-63.
37. Baliga, B. and S. Kumar, *Apaf-1/cytochrome c apoptosome: an essential initiator of caspase activation or just a sideshow?* Cell Death Differ, 2003. **10**(1): p. 16-8.
38. Spataro, V., C. Norbury, and A.L. Harris, *The ubiquitin-proteasome pathway in cancer.* Br J Cancer, 1998. **77**(3): p. 448-55.
39. Schlossarek, S. and L. Carrier, *The ubiquitin-proteasome system in cardiomyopathies.* Curr Opin Cardiol, 2011. **26**(3): p. 190-5.
40. Dai, C. and W. Gu, *p53 post-translational modification: deregulated in tumorigenesis.* Trends Mol Med, 2010. **16**(11): p. 528-36.
41. Carson, J.A. and K.A. Baltgalvis, *Interleukin 6 as a key regulator of muscle mass during cachexia.* Exerc Sport Sci Rev, 2010. **38**(4): p. 168-76.
42. Acharyya, S., et al., *Cancer cachexia is regulated by selective targeting of skeletal muscle gene products.* J Clin Invest, 2004. **114**(3): p. 370-8.
43. Tisdale, M.J., *Mechanisms of cancer cachexia.* Physiol Rev, 2009. **89**(2): p. 381-410.
44. Fodde, R., *The APC gene in colorectal cancer.* Eur J Cancer, 2002. **38**(7): p. 867-71.
45. Baltgalvis, K.A., et al., *Activity level, apoptosis, and development of cachexia in Apc(Min/+) mice.* J Appl Physiol, 2010. **109**(4): p. 1155-61.
46. Baltgalvis, K.A., et al., *Interleukin-6 and cachexia in ApcMin/+ mice.* Am J Physiol Regul Integr Comp Physiol, 2008. **294**(2): p. R393-401.
47. Tessitore, L., et al., *Cancer cachexia, malnutrition, and tissue protein turnover in experimental animals.* Arch Biochem Biophys, 1993. **306**(1): p. 52-8.
48. White, J.P., et al., *Muscle oxidative capacity during IL-6-dependent cancer cachexia.* Am J Physiol Regul Integr Comp Physiol, 2011. **300**(2): p. R201-11.
49. Kandarian, S., et al., *Regulation of skeletal muscle dihydropyridine receptor gene expression by biomechanical unloading.* J Appl Physiol, 1992. **72**(6): p. 2510-4.

50. Costelli, P., et al., *Activation of Ca(2+)-dependent proteolysis in skeletal muscle and heart in cancer cachexia.* Br J Cancer, 2001. **84**(7): p. 946-50.
51. Fujita, J., et al., *Anti-interleukin-6 receptor antibody prevents muscle atrophy in colon-26 adenocarcinoma-bearing mice with modulation of lysosomal and ATP-ubiquitin-dependent proteolytic pathways.* Int J Cancer, 1996. **68**(5): p. 637-43.
52. Strassmann, G., et al., *Mechanisms of experimental cancer cachexia. Local involvement of IL-1 in colon-26 tumor.* J Immunol, 1993. **150**(6): p. 2341-5.
53. Wysong, A., et al., *NF-kappaB inhibition protects against tumor-induced cardiac atrophy in vivo.* Am J Pathol, 2011. **178**(3): p. 1059-68.
54. Mandel, I.D., C.E. Barr, and L. Turgeon, *Longitudinal study of parotid saliva in HIV-1 infection.* J Oral Pathol Med, 1992. **21**(5): p. 209-13.
55. Zhang, H., et al., *Role of interleukin-6 in cardiac inflammation and dysfunction after burn complicated by sepsis.* Am J Physiol Heart Circ Physiol, 2007. **292**(5): p. H2408-16.
56. Kelly, M., et al., *AMPK activity is diminished in tissues of IL-6 knockout mice: the effect of exercise.* Biochem Biophys Res Commun, 2004. **320**(2): p. 449-54.
57. Latronico, M.V., et al., *Regulation of cell size and contractile function by AKT in cardiomyocytes.* Ann N Y Acad Sci, 2004. **1015**: p. 250-60.
58. Castedo, M., K.F. Ferri, and G. Kroemer, *Mammalian target of rapamycin (mTOR): pro- and anti-apoptotic.* Cell Death Differ, 2002. **9**(2): p. 99-100.
59. Yang, E., et al., *Bad, a heterodimeric partner for Bcl-XL and Bcl-2, displaces Bax and promotes cell death.* Cell, 1995. **80**(2): p. 285-91.
60. Zha, J., et al., *Serine phosphorylation of death agonist BAD in response to survival factor results in binding to 14-3-3 not BCL-X(L).* Cell, 1996. **87**(4): p. 619-28.
61. Egan, D., et al., *The autophagy initiating kinase ULK1 is regulated via opposing phosphorylation by AMPK and mTOR.* Autophagy, 2011. **7**(6).
62. Tian, M., et al., *Cardiac alterations in cancer-induced cachexia in mice.* Int J Oncol, 2010. **37**(2): p. 347-53.
63. Xu, H., et al., *Myocardial dysfunction in an animal model of cancer cachexia.* Life Sci, 2011. **88**(9-10): p. 406-10.
64. Barcena Roji, L., et al., *[Dental prevention in the geriatric patient].* Rev Actual Estomatol Esp, 1989. **49**(386): p. 59-60, 63-4.
65. Dillmann, W.H., *Methyl palmoxirate increases Ca2+-myosin ATPase activity and changes myosin isoenzyme distribution in the diabetic rat heart.* Am J Physiol, 1985. **248**(5 Pt 1): p. E602-6.
66. Morris, G.S., M.C. Prevost, and A.G. Nelson, *Morderate diabetes alters myosin isoenzyme distribution in cardiac but not skeletal muscle of male rats.* Life Sci, 1996. **58**(10): p. 833-8.
67. Reiser, P.J., et al., *Human cardiac myosin heavy chain isoforms in fetal and failing adult atria and ventricles.* Am J Physiol Heart Circ Physiol, 2001. **280**(4): p. H1814-20.
68. Nakanishi, K., et al., *Changes in myosin heavy chain and its localization in rat heart in association with hypobaric hypoxia-induced pulmonary hypertension.* J Pathol, 2002. **197**(3): p. 380-7.